

## DESIGN PHASE OF A CYLINDRICAL LONG-SPAN COAL SHED WITH STEEL ARCH SPACE-TRUSS STRUCTURE

Angga Fajar Setiawan<sup>1\*</sup>, Akhmad Aminullah<sup>1</sup>, Ali Awaludin<sup>1</sup>, K. T. N., Gherry<sup>1</sup>, Y. A. Adhitama<sup>1</sup>, and M. Fauzi Darmawan<sup>1</sup>

<sup>1</sup>Departemen Teknik Sipil dan Lingkungan, Universitas Gadjah Mada, Jl. Grafika no. 2, Yogyakarta  
Email: [Angga.fajar.s@ugm.ac.id](mailto:Angga.fajar.s@ugm.ac.id)

### ABSTRACT

This paper discusses the structural design phase of a long-span coal shed structure in a 2x50 MW steam power plant. This study aims to share knowledge on how to design a long-span coal shed structure safely based on the design standards. The main structural system of the coal shed roof is a steel arch space-truss with 120 m of span and 31 m of height above supporting 12.5 m height of reinforced concrete columns. The superstructure contains a roof system and a reinforced concrete system. The substructure system consists of a tie beam, pile cap, and bore pile. In the numerical model, all structural members were idealized as frame elements, except the pile cap that to be idealized as shell elements. Then, the soil springs were assigned to the bore pile element nodes with a 1 m interval to simulate the soil-structure interaction. The gravity loads due to dead loads, additional dead loads, live loads, rain loads, and lateral loads due to wind action and earthquakes to be considered. Furthermore, the structural analysis was conducted with non-linear geometric to simulate the large displacement effects and tension only element of the wind bracing. In addition, a simplified method to estimate the structural stability under lateral load was conducted. Based on the structural analysis and structural design, the coal shed structure could fulfill the safety criteria in terms of ultimate and serviceability limit based on the design code criteria. Furthermore, the non-linear geometry and stability issue should be considered with an appropriate structural analysis method.

Keywords: long span coal shed, arch space-truss, steel structure, structural design

### 1. INTRODUCTION

In a developing country, the demand for electrical energy spurs power plant construction. One of the alternatives is the steam power plant with coal-fired fuel. Coal-fired is the world's major fuel for electrical power generation (IEA, 2014) because of the extensively disseminated and low-cost fuel (IEA, 2012). On the steam power plant site, before the coal is fired, it needs to be stored in a coal yard. To prevent the decrement of the coal's calories due to the wetting process (Bhatt and Labs, 2016), the coal shed is needed in keeping the low moisture content. The coal shed structural span length should be sufficient to accommodate the mound of coal and the stacker reclaimers machine below. Regarding the long span and the room space demand of the coal shed, the steel arch space-truss structural system is the fit alternative. The arch space-truss configuration has several benefits for long-span structure i.e., sufficient vertical stiffness to reduce the vertical displacement, converting large bending moment with the axial internal force action of element members, aesthetic view of structural system, a minimal amount of material demand, and achievable building cost (Du *et al.*, 2017) (Hladik and Lewis, 2010). Several predecessor studies have discussed the structural design of long-span coal sheds. The structural optimization of long-span cylindrical space-truss for dry-coal-shed has been conducted in Liyuan of Henan province (Du *et al.*, 2017). That structure was designed with two layers of space-truss to tend 155.6 m span length. The other study that discussed the long-span structure is the Singapore National Stadium dome roof (Hladik and Lewis, 2010). The structure is designed with an asymmetric shape and has 6 arches span with 312 m of diameter. However, there were some failures of long-span roof structures under construction that occurred in Indonesia dominantly due to the lack of competence in understanding structural design and stability concepts and inappropriate construction methods (Dewobroto, 2021). There has not been a detailed discussion paper about the procedures and the important points about preserving structural safety during the design phase. A lesson of the correct experience structural design of long-span coal shed needs to be shared on the structural engineering knowledge.

This paper explains the structural design stage of a long-span coal shed structure in a 2x50 MW steam power plant. The principal structural system of the coal shed roof is an arch space-truss (triangular formation of steel pipe section) with 120 m of span, 31 m of height, and 75.8 m of radius. The substructure is composed of the bore pile, pile cap, and tie beam. The arch space-truss is configured 14 spans at 7 m along the longitudinal direction of the coal shed, as illustrated in Figure 1. The spans of the main arch structure are connected by vertical bracing and wind bracing combined with longitudinal stiffener parallel with the longitudinal direction of the coal shed, as illustrated in Figure 2 (a) and (b). The arch structure is supported by reinforced concrete columns with a height of 12.5 m from ground

Corresponding Author

E-mail Address : [angga.fajar.s@ugm.ac.id](mailto:angga.fajar.s@ugm.ac.id)

level. In the design process, the calculated loads are gravity loads due to dead loads, additional dead loads, live loads, rain loads, lateral loads due to wind load (115.6 km/h), and earthquakes load (2% probability in 50 years of spectra design) for the Kupang area. The structural analysis was conducted with a three-dimensional (3D) numerical model. In addition, non-linear geometric to accommodate the large displacement effects and tension only element of the wind bracing. There are two earthquake load analysis methods to be implemented i.e., equivalent static and modal response spectrum. Furthermore, a simplified numerical model of the main space-truss, longitudinal stiffener, and wind bracing structural system to estimate the structural stability under lateral load to be conducted. The structural design concept of the coal shed discussion is expected to serve engineering experience on how to design a long-span coal shed structure safely according to the applicable design standards.

## 2. STRUCTURAL CONFIGURATION

The major components of the coal shed structure consist of the superstructure and substructure. The superstructure contains a roof and reinforced concrete (RC) moment resisting system, as depicted in Figure 2 (a) and (b). The roof structure is composed of the main arch space-truss, and lateral resisting system i.e., vertical bracing, longitudinal stiffener with steel pipe section, and wind bracing, as depicted in Figure 3. The main arch space-truss cross-section is configured as a triangular formation of steel pipe, as depicted in Figure 3 (b) and (c). It contains one arch bottom member with 10” of diameter, two arch top members with 6” of diameter, and diagonal members with 4” of diameter. The vertical bracing connects the arch space-truss in interval 20 m with fix connection system. In addition, the wind bracing is contained of the bar section with diameter 16 mm and 22 mm. Then, the longitudinal stiffener member is made of the steel pipe section with 4” of diameter. Moreover, the typical section of the roof structural members is shown in Table 1. The reinforced concrete (RC) supporting system consists of columns and ring balks with cross-section dimensions 1.5x1.8 m<sup>2</sup> and 0.75x1.0 m<sup>2</sup>, respectively. Finally, the substructure system is reinforced concrete structures consisting of a tie beam, pile cap, and bore pile with 1.8x1.0 m<sup>2</sup> of area, 1.4 m of thickness, and 0.6 m of diameter, respectively, as illustrated in Figure 2 (a).

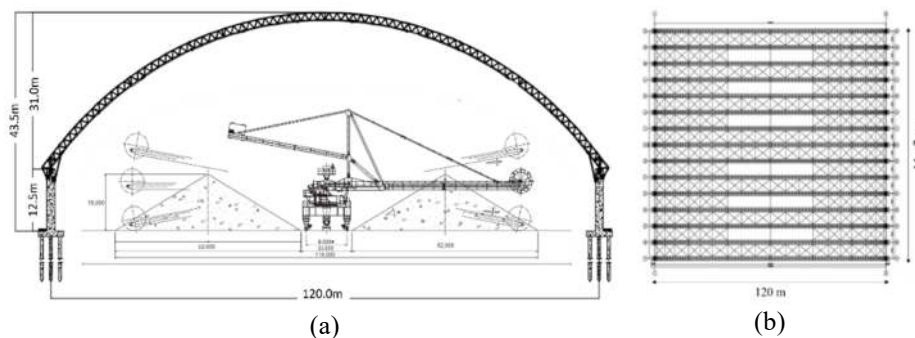


Figure 1. The layout of the dry-coal-shed structure.

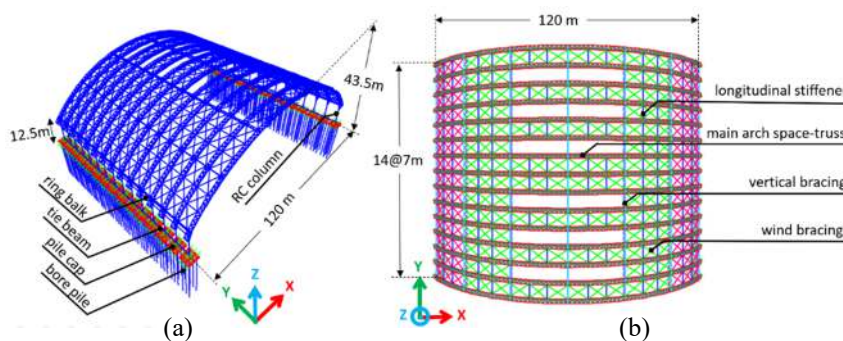


Figure 2. (a) Idealization 3D model of the structure and (b) top view of the structural model.

## 3. STRUCTURAL ANALYSIS METHOD

In the structural analysis, the numerical model coal shed structure was developed with three-dimensional (3D). The numerical model of the superstructure was idealized as a frame element, as illustrated in Figure 2 (a) and (b). The element's end of steel arch space-truss, vertical bracing, and longitudinal stiffener to be idealized as fix connection (unreleased moment) because of the implementation of stiffener plate in welding connection and tightened and massive configuration of bolt connection joint. Furthermore, the wind bracing element (bar section) as infill in the void of the main space-truss and longitudinal stiffener to be idealized as a tension-only element due to the extremely

slender member. Then, the reinforced concrete moment-resisting frame system consists of the column and ring balk also to be idealized as frame element. In addition, to control the safety member of bore pile member and more realistic support stiffness, the substructure structural system was also modeled. The pile cap was idealized as a shell element and the tie beam and bore pile foundation (23.5m of depth) to be idealized as a frame element. To consider the stiffness effect of the soil bearing to the bore pile, soil spring is added in the bore pile element.

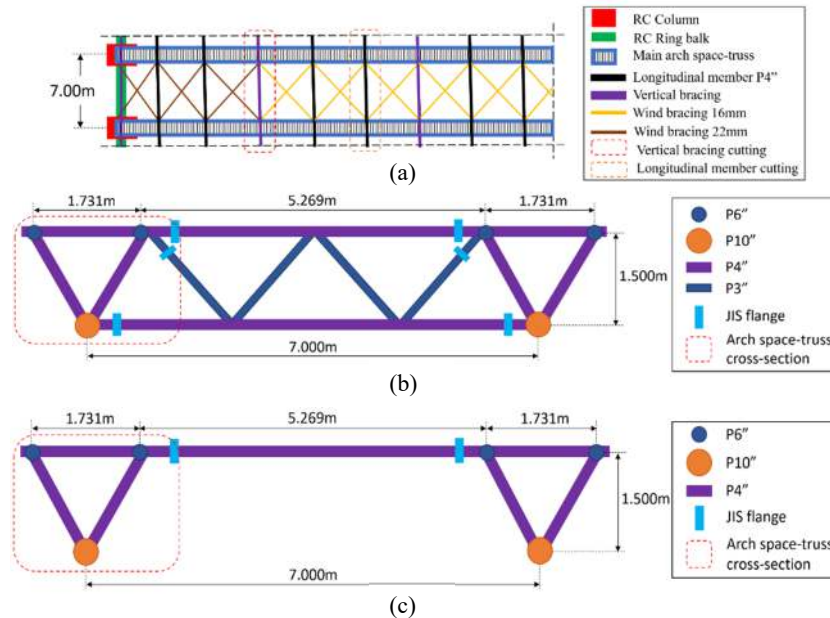


Figure 3. The detailed structural configuration of steel roof: (a) top view of main arch space arch with wind bracing and longitudinal member, (b) cut view of main arch space-truss cross-section with vertical bracing, and (c) cut view of main arch space-truss cross-section with longitudinal stiffener.

The numerical analysis of the structural model implements a direct stiffness matrix for the frame element and finite element formulation for the shell element. The equilibrium concept between the external and internal force in the direct stiffness of the matrix method is expressed in Equation (1). In the local coordinate, both the frame element and shell element contain six degrees of freedom (DOF). To simulate the non-linear geometric effect of the long-span coal shed structure, the numerical modeling also considers P-Delta with large displacement which the element stiffness matrix is formulated in Equation (2), based on the reference (Yang and Asce, 1986). Where,  $\{F\}$  is the global force matrix-vector,  $[K]$  is the global stiffness matrix,  $\{U\}$  is the global displacement matrix-vector,  $\{^2f\}$  is the element force matrix-vector in end increment,  $\{^1f\}$  is the element force matrix-vector in the previous of end increment,  $\{k_e\}$  is the elastic stiffness matrix of element,  $\{k_g\}$  is the geometric stiffness matrix of element, and  $\{u\}$  is the displacement matrix of element.

$$\{F\} = [K]\{U\} \quad (1)$$

$$\{^2f\} - \{^1f\} = [k_e]\{u\} + [k_g]\{u\} \quad (2)$$

### Materials and Section Properties

The steel material of the roof structure implements the ASTM A53 grade B, the minimum yield strength and tensile strength are 240 MPa and 415 MPa, respectively. The reinforced concrete columns, ring balk, tie beam, and pile cap implement concrete material with the compressive strength of 30 MPa. Then, the bore pile foundation member implements concrete material with compressive strength of 25 MPa. Furthermore, the rebar for the concrete reinforcement minimum yield strength is 420 MPa.

### Soil-Structure Interaction

In this study, the soil-structure interaction (FEMA, 2020) was considered in the structural numerical model. For soil parameters, we input the modulus of subgrade reaction ( $K_S$ ) value (E. Bowles, 1997). In this study, soil lateral resistance is modeled as a spring element that is assigned in each 1 m interval of the bore pile height, as depicted in Figure 4. The spring element adopted in the calculation follow Winkler's spring theory as expressed in Equation (3)-

(5). There is two translation degree of freedom components of spring, i.e. vertical soil spring ( $K_{sv}$ ) and lateral soil spring ( $K_{sh}$ ).

Table 1. Section properties of roof structural members

Name of structural group	Position	Dimension
Main arch space-truss	Top member	Pipe 6" (P3)
	Bottom member	Pipe 10" (P10)
	Diagonal member	Pipe 4" (P4)
Vertical bracing	Top and bottom member	Pipe 4" (P4)
	Diagonal member	Pipe 3" (P3)
Wind bracing	Bar	Ties 16 mm and 22 mm
Longitudinal member	Longitudinal member	Pipe 4" (P4)

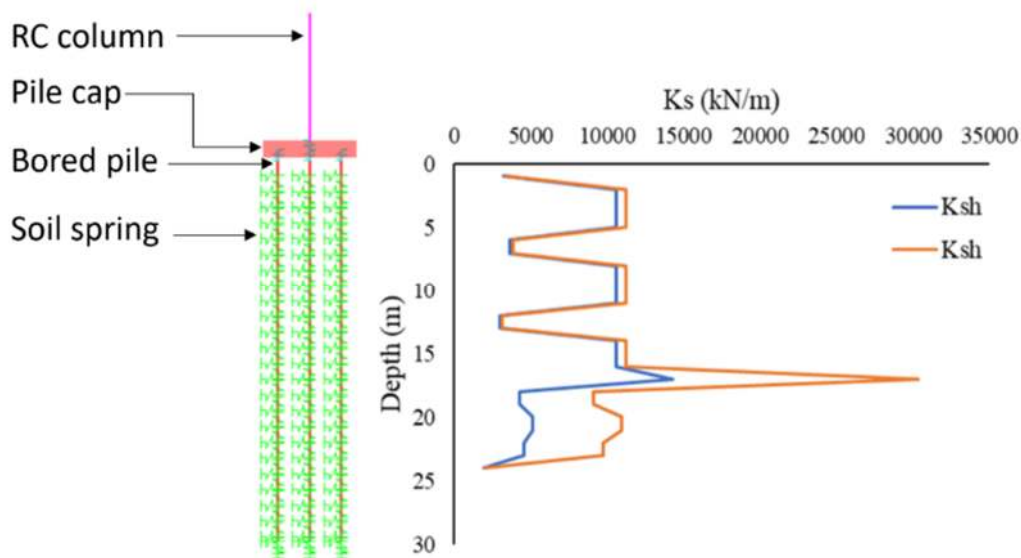


Figure 4. The structural idealization of the foundation system

$$C_u = 6.25 N_{SPT} \tag{3}$$

$$K_{Sv} = 120 C_u \text{ (KN / m}^3\text{)} \tag{4}$$

$$\text{for clay soil, } K_{Sh} = K_{Sv}, \text{ and for sand soil, } K_{Sh} = 2K_{Sv} \tag{5}$$

### Gravity Load (Dead, Additional Dead, Rain, and Roof Lives)

Dead load is the weight of all constructed structural material of members, according to the loading standard (BSN, 2020a). In numerical modeling, it is automatically calculated and assigned distributed on the structural element by the structural analysis software, as illustrated in Figure 5 (a). The steel material and reinforced concrete material unit weight input to be assumed 78.5 KN/m<sup>3</sup> and 24 KN/m<sup>3</sup>.

In addition, the additional dead load is the gravity load from the weight of the non-principle structural member. The additional dead loads that manually to be assigned distributed on element members and concentrated on the structural joint, as depicted in Figure 5 (a). The additional dead load consists of joint and connection of steel structure with 10 kg of weight, purlin with 9.27 kg/m of weight per unit length, roof with 5.1 kg/m<sup>2</sup> of weight per unit area (Lysaght Zinalume steel), the mechanical-electrical with the total weight per area is 5 kg/m<sup>2</sup>.

Based on the structural loading standard (Departemen Pekerjaan Umum, 1987), the magnitude of rain load was determined as (40-0.8 $\alpha$ ) kg/m<sup>2</sup>, while the load does not greater than 20 kg/m<sup>2</sup>. The  $\alpha$  is the angle of roof slope in degree. If the roof slope is greater than 50<sup>0</sup>, then the rain load does not need to be calculated. The rain load was assigned on element nodal where the purlin is supported, as depicted in Figure 5 (a).

The roof lives load ( $L_r$ ) was considered as the provision of the loading standard code BSN (2020a) and ICC (2017). As per the mentioned code, the magnitude of the roof live load shall be in the range between 0.58 to 0.96 kN/m<sup>2</sup>. The

load reduction factor to be considered as the tributary area and geometric of the coal shed roof, the magnitude of the  $L_r$  is  $0.45 \text{ kN/m}^2$ . When following the minimum limit criteria, therefore, the  $L_r$  should be  $0.58 \text{ kN/m}^2$ .

### Wind Load (W)

In the long-span structure, such as the coal shed, the wind load will trigger a major threat to structural stability and safety. Therefore, the proper magnitude of wind load design should be considered well. The basic wind speed ( $V_{50}$ ) which is defined as a 3 s gust at 10 m height in flat open country terrain, corresponding to 50 year return period (Halmes and Weller, 2002) was determined. Then, the wind loads magnitude was calculated according to BSN (2020a) and ASCE (2017), as expressed in Equation 6. The wind load parameters input is listed in Table 2. It should be assigned in both transversal (X) and longitudinal (Y) directions, as illustrated in Figure 5 (b).

On the lateral (X) direction of the coal shed structure, the wind pressure distribution is composed of the compression in the arrival side surface and the suction leave side following BSN (2020a), as illustrated in Figure 5 (c). Furthermore, in the longitudinal (Y) direction of the coal shed, the pressure deployment is the compression only. The projection area of wind pressure on the longitudinal direction to be assumed one-third the area of the arch-space truss in longitudinal view, following the standard for bridge load (BSN, 2006). The wind pressure in Equation (6) was converted as load and to be assigned in each joint of the roof structure, as depicted in Figure 5 (d). Where  $q_z$  is velocity pressure on z level, then  $K_z$  is velocity pressure exposure coefficient,  $K_{zt}$  is a specific topographic factor, and V is base wind speed (on m/s).

$$q_z = 0.613K_zK_{zt}K_dV^2 \text{ (N/m}^2\text{)} \quad (6)$$

Table 2. Wind load parameters

Wind load parameters	Value	Wind load parameters	Value
Basic wind speed	115.6 km/h	$G_{epi}$ for open building	0
Wind direction factor ( $K_D$ )	0.85	$C_p$ ¼ windward	0.3
Exposure factor	C	$C_p$ ½ center of the roof	-0.96
Topography factor ( $K_{zt}$ )	1	$C_p$ ¼ leeward	-0.5
Gust effect factor (G)	0.85	Distance between column	7 m

### Earthquake Load (E)

In the structural design of the coal shed, two earthquake analysis methods were implemented i.e., equivalent static and modal response spectrum. The equivalent static (ES) to being applied because it is more conservative and the procedure is easy to be estimated and interpreted. Besides that, the non-linear analysis could be conducted with an equivalent static method in considering a tension-only element of the wind bracing which uses the extremely slender member of the bar section. Generally, the modal response spectrum (RS) is the most ideal method for the structural design, because the method is automatic, simple and it could consider the dynamic behavior of the structure (modal analysis) in distributing the seismic load. However, this method could not cover the non-linear analysis to simulate tension-only elements. Therefore, the implementation of two methods of earthquake analysis is expected could assure structural safety among the lack of each method with a remain affordable analysis.

In term of the applied earthquake force magnitude, the seismic load magnitude to the coal shed structure high possibility not in peak spectra, because of the long natural period of the structure, as illustrated in Figure 5 (e). However, generally, the long span has less stability than the normal span structure under lateral load. Therefore, the lateral stabilizer system needs to be added i.e., the vertical bracing, longitudinal member combined with wind bracing. In addition, the response modification factor (R) adjustment for long-span structure should be determined properly according to BSN (2019) and ASCE (2017). The coal shed structure is categorized as a non-building similar to a building. In this study, the seismic modification factor for the roof structural system to be assumed 2.5 and for the reinforced concrete structure to be determined as 3.0. The roof structural system was idealized as the ordinary steel concentrically braced frame with a permitted additional height limit. Then, the reinforced concrete structural system is designed as the ordinary moment resisting frame with a permitted additional height limit. Furthermore, the value of the system overstrength factor ( $\Omega_0$ ) and deflection magnification factor ( $C_d$ ) for both of roof structural system and RC supporting system are 2.0 and 2.5, respectively.

The response spectra design is determined based on the Indonesian Earthquake Hazard Map 2017 (Pustlitbang PUPR, 2017). The coal shed structure is located in Kupang, Indonesia, with site type being medium soil. Then, the risk category of coal shed structure is in class III, because the structure is categorized as an ordinary power plant's facility. Therefore, the importance level factor of the coal shed structure is 1.25. According to the soil test data and BSN

(2019), the seismic design category for the coal shed structure is D. Finally, the input parameters of earthquake response spectra design and the graph are shown in Table 3 and Figure 5 (f), respectively.

#### 4. STRUCTURAL SAFETY CRITERIA

In this study, to assure structural safety, the coal shed structure should fulfill the serviceability limit and ultimate limit state criteria. The serviceability limit is adopted in assessing the structural displacement and verification of the soil resistance of foundation safety with the allowable stress design (ASD) concept. According to the structural design standard code BSN (2020c) and AISC (2020), on the ultimate limit criteria, the strength of the structural system, structural members, and foundation elements should be designed equal or beyond the internal force of the factored load combinations in the load resistance factor design (LRFD), as expressed in Equation (7). Where,  $\phi$  is the strength reduction factor,  $R_n$  is the nominal strength of the structural members, and  $R_u$  is the internal force response of the member under factored load combination that consists of dead load, roof live load, rain load, wind load, and earthquake load. In the serviceability limit criteria, the load types to be combined without load factor, as the ICC (2017) and BSN (2020a). While, in the ultimate limit state combination criteria, the load types should be factored. The considered load combinations of the coal shed structural design are listed in Table 4.

$$R_u \leq \phi R_n \tag{7}$$

Table 3. Input parameter of response spectra design

No.	Earthquake parameters	Value	No.	Earthquake parameters	Value
1	$S_s$	1.10	7	$S_{DS}$	0.77
2	$S_1$	0.25	8	$S_{D1}$	0.35
3	$F_a$	1.06	9	$T_s$	0.45
4	$F_v$	2.10	10	$T_0$	0.09
5	$S_{MS}$	1.166	11	$S_{a0}$	0.31
6	$S_{M1}$	0.53			

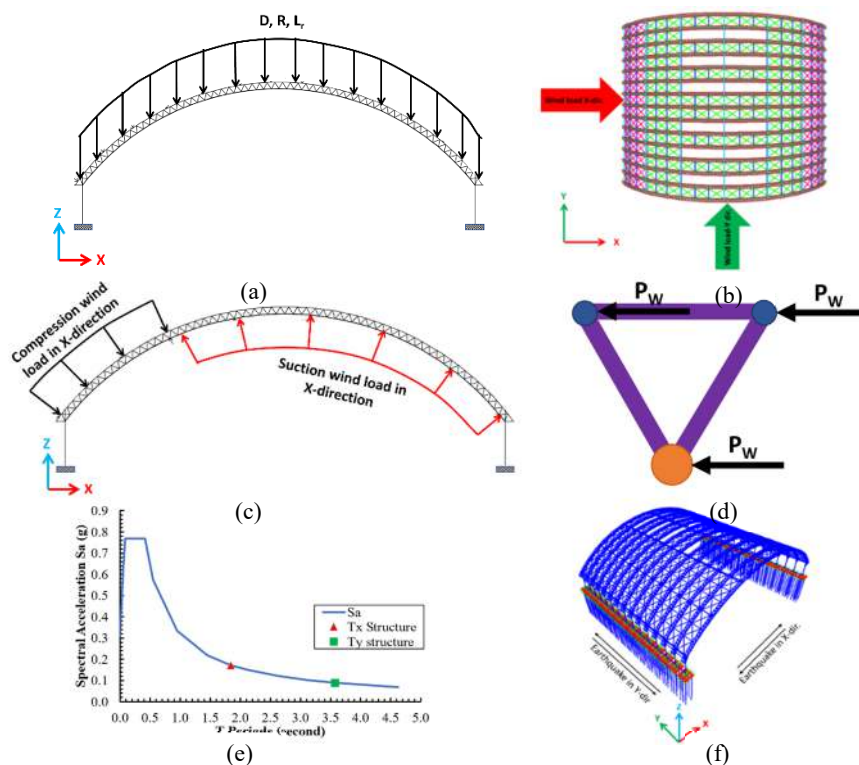


Figure 5. Structural loading: (a) dead load (D), additional dead load (AD), and rain load (R) assignment, (b) wind loads (W) in global view, (c) wind load assignment in X-axis direction, (d) wind assignment load in Y-axis direction, (e) response spectra design, and (f) earthquake load (E).

## 5. STRUCTURAL RESPONSE AND STRUCTURAL DESIGN

After all structural loading is assigned to a structural model member, the reasonable structural response needs to be verified. In this study, we monitored the predominant structural vibration mode shape, displacement, and base reaction. After the structural response was verified with a reasonable result, the structural member's design will be conducted. The structural system and element member should comply with the safety criteria in serviceability and ultimate limit according to the standard codes. In this study, we limited the structural design to only the steel roof structural system.

### Predominant Vibration Mode Shape

The modal analysis was conducted to capture the structural vibration mode shape, especially the predominant vibration mode shape with the natural period of the structure. The vibration mode shape structure is one of the structural dynamic properties that represent the balance point of structural stiffness and mass. In this study, 1000 structural mode shapes were searched with the Eigen solver method to achieve a minimum of 90% of mass participating ratio according to seismic minimum criteria of the seismic standard code of BSN (2019) and ASCE (2017). The modal analysis was conducted with dead load (D) analysis in the structural initial state. Since the wind bracing is the tension-only member in the real, while the modal analysis capability only in linear analysis (the tension-only element model could not proceed). The deletion of one member in the pair wind bracings needs to be conducted to represent the absence of its compression occurrence (named as SM1). Based on the modal analysis, the 95% mass participation could be achieved at 998<sup>th</sup> and 999<sup>th</sup> of modes in the transverse and longitudinal direction, respectively. This structural model (SM1) was also adopted for the modal response spectrum (RS) analysis of earthquake load. While the equivalent static analysis (ES) remains to implement a full wind bracing model with tension-only element assignment (named as structural SM2).

The results of the mode shape and structure period from the modal analysis are shown in Figure 6. We can see that the structure had a translation-translation-rotation mode shape. The first mode of SM1 and SM2 was translation motions on the longitudinal (Y-axis) direction with 3.575 s and 2.845 s of the natural period, respectively. Then, the second mode of them was translation motion on the transversal (X-axis) direction with 1.837 s and 1.835 s of the natural period, respectively. Furthermore, the third mode of structure is rotational motion with 1.780 s and 1.765 s of the natural period, respectively. As the comparison of the structural model SM1 and SM2, the deletion of one member in a pair of wind bracing could generate a significant difference in the 1<sup>st</sup> structural mode shape. It can be noted that the modeling wind bracing in a steel structural system should consider the tension-only effect with a proper structural idealization adjustment.

Table 4. The load combinations

Type of loads	ASD	LRFD
	D	1.4D
	D + (L <sub>r</sub> or R)	1.2D + 0.5(L <sub>r</sub> or R)
	D + 0.75(L <sub>r</sub> or R)	1.2D + 1.6(L <sub>r</sub> or R) + 0.5W
Combinations	D + (0.6W or 0.7E <sub>v</sub> + 0.7E <sub>mh</sub> )	1.2D + 1.0W + 0.5(L <sub>r</sub> or R)
	D + 0.525W + 0,75(L <sub>r</sub> or R)	0.9D + 1.0W
	D + 0.525(E <sub>v</sub> + E <sub>mh</sub> )	1.2D + E <sub>v</sub> + E <sub>h</sub>
	0.6D + (0.6W or 0.7E <sub>v</sub> + 0.7E <sub>mh</sub> )	0.9D + E <sub>v</sub> + E <sub>h</sub>

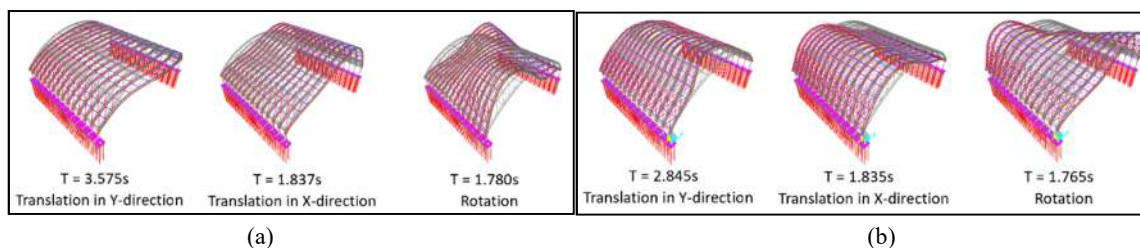


Figure 6. The 1st, 2nd, and 3rd structural mode shapes: (a) SM1 and (b) SM2.

**Displacement**

The vertical deflections of arch space-truss under  $L_r$ , R or W, and  $D+L_r$  were controlled based on the ICC (2017) with a limit is  $l/180$ ,  $l/180$ , and  $l/120$ , respectively, where the  $l$  is the arch span. When the arch space-truss span is 120m, the deflection limits are 667 mm, 667 mm, and 1000 mm based on the  $l/180$  and  $l/120$  criteria, respectively. The rain load (R) substitutes the snow load (S) to adapt the steel roof structure located in tropical areas. The structural analysis without considering P-delta with large displacement was also conducted as comparer.

As the numerical analysis, the maximum vertical deflections ( $\Delta_v$ ) in the middle span of the main space-truss under  $L_r$ , R, and  $D+L_r$  are shown in Table 5. We could observe that the vertical displacement with and without considering non-linear geometric fulfill the ICC (2017) criteria. The vertical deflections with considering non-linear geometric resulted in around 33% larger than the unconsidered one in the case  $D+L_r$ . While, under smaller load case ( $L_r$  or R), the structural displacement by considering non-linear geometric almost equal value with only linear geometric.

Under wind load, the maximum lateral displacements of the space-truss are in transversal (X), longitudinal (Y), and vertical (Z) are 134.5, 75.2, and 363.8 mm, respectively. It remains below the limit criteria following the IBC 2018 (ICC, 2017), as listed in Table 6. The effect of non-linear geometric resulted in a slight difference of displacement magnitude.

Under earthquake load, the lateral displacement of the steel arch space-truss and the RC supporting system remain below the limit criteria of the seismic standard, as shown in Table 7 and Table 8. Those lateral displacements have been multiplied by magnification factor  $C_d$  and divided by the importance factor (I), according to the earthquake load standard (BSN, 2019). The displacement limit of arch space-truss in transversal (X) direction and longitudinal (Y) direction to be determined based on the 1.5% of the arch space-truss height ( $h_r$ ) and span length ( $l$ ), respectively. While the lateral displacement limit of the RC supporting system is based on 1.5% of the column height ( $h_c$ ). Compared with the unconsidered non-linear geometric effect in the numerical analysis in seismic load analysis, its effect is not a significant value to the lateral displacement. In addition, the response spectrum analysis generated in the smaller displacement response the equivalent static seismic load analysis, except in the case of the RC column response on longitudinal (Y) direction.

Table 5. Vertical displacement ( $\Delta_v$ , mm) control of the steel roof structural system

Analysis Consideration	$L_r$	$l/180$	Control	R	$l/180$	Control	$D+L_r$	$l/120$	Control
Non-linear geometric	137.4	666.7	Fulfill	89.6	666.7	Fulfill	367.4	1000.0	Fulfill
Linear geometric	136.9		Fulfill	89.4		Fulfill	276.2		Fulfill

Table 6. Displacement ( $\Delta$ , mm) control of the steel roof structural system under wind load

Analysis Consideration	$W_x$	$l/180$	Control	$W_y$	$l/180$	Control	$W_z$	$l/180$	Control
Non-linear geometric	134.5	666.7	Fulfill	75.2	666.7	Fulfill	363.8	666.7	Fulfill
Linear geometric	137.2		Fulfill	75.1		Fulfill	370.7		Fulfill

Table 7. Horizontal displacement ( $\Delta_h$ , mm) control of the steel roof structural system under earthquake

Analysis Consideration	$E_{x,ES}$	$E_{x,RS}$	$1.5\%h_r$	Control	$E_{y,ES}$	$E_{y,RS}$	$1.5\%l$	Control
Non-linear geometric	272.6	-	465.0	Fulfill	465.6	-	1800.0	Fulfill
Linear geometric	273.8	68.6		Fulfill	465.0	351.2		Fulfill

Table 8. Horizontal displacement ( $\Delta_h$ , mm) control of the reinforced concrete column

Analysis Consideration	$E_{x,ES}$	$E_{x,RS}$	$1.5\%h_c$	Control	$E_{y,ES}$	$E_{y,RS}$	$1.5\%h_c$	Control
Non-linear geometric	58.6	-	187.5	Fulfill	18.4	-	187.5	Fulfill
Linear geometric	58.58	44.4		Fulfill	18.4	32.6		Fulfill

**Base Reactions**

According to the structural analysis, the base reaction of the structure under equivalent static (ES) seismic load analysis is listed in Table 9. Compared with the dead load (D) that acts as a mass, the seismic base reaction is in the range of 7% to 9% for the transversal (X) direction. While in the longitudinal (Y) direction the base reaction is around 4% g. When we calculate the seismic acceleration factor (CI/R) manually, the transversal (X) and longitudinal (Y) direction



should have 8.61% g and 4.43% g, respectively. For the RC structural supporting system, it should have 7.17% g and 3.69%. Therefore, the ES seismic analysis method validity was verified. Then, the base reaction of the ES method was adopted as the control of the response spectrum method, as the provision of codes (ASCE, 2017)(BSN, 2019).

Table 9. Base reactions control

Structural system	Base shear (kN)		Base shear (% g)	
	Lateral (X)	Longitudinal (Y)	Lateral (X)	Longitudinal (Y)
Steel roof (R = 2.5)	9785.58	5058.09	8.62%	4.45%
RC supporting structure (R = 3.0)	8154.65	4851.28	7.18%	4.27%
Dead load (D)	113538.74		100.00%	

### Structural Member Design Control

In the structural design, the primary structural member safety for load resistance was controlled with the demand/capacity (D/C) ratio. Under the individual type of the internal force, the demand capacity ratio of the structural member should comply with Equation (7). Then, under the interaction of axial-moment internal force, the structural member should fulfill safety criteria when the demand capacity (D/C) ratio should equal to or less than 1.0 (BSN, 2020c), as expressed in Equation (8). The results of demand capacity ratios control of the steel roof structural system are depicted in Table 10. All structural members complied with the safety criteria. It can be monitored that the most critical load demand arose from the contained earthquake load and wind load combination. The modal analysis response spectrum (RS) seismic analysis inflicted the most severe structural member internal force. While the structural safety level was firm under the only contained gravity load combination.

$$\text{For } \frac{P_u}{P_n} < 0.2, \frac{P_u}{2P_n} + \left( \frac{M_{u22}}{M_{n22}} + \frac{M_{u33}}{M_{n33}} \right) \leq 1 \text{ and for } \frac{P_u}{P_n} \geq 0.2, \frac{P_u}{P_n} + \frac{8}{9} \left( \frac{M_{u22}}{M_{n22}} + \frac{M_{u33}}{M_{n33}} \right) \leq 1 \quad (8)$$

Table 10. The maximum demand/capacity (D/C) ratios of the steel roof structural members

Structural member section	D/C of P-M under ultimate load combination			
	Gravity load only	Contained W	Contained ES load	Contained RS load
Pipe 10"	0.638	0.963	0.840	0.798
Pipe 6"	0.542	0.806	0.731	0.966
Pipe 4"	0.121	0.352	0.431	0.880
Pipe 3"	0.057	0.089	0.178	0.261

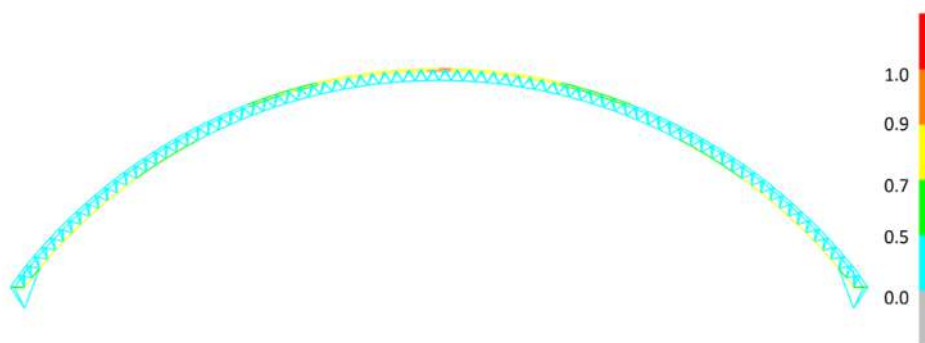


Figure 7. The distribution demand capacity ratio of the main arch space-truss structure

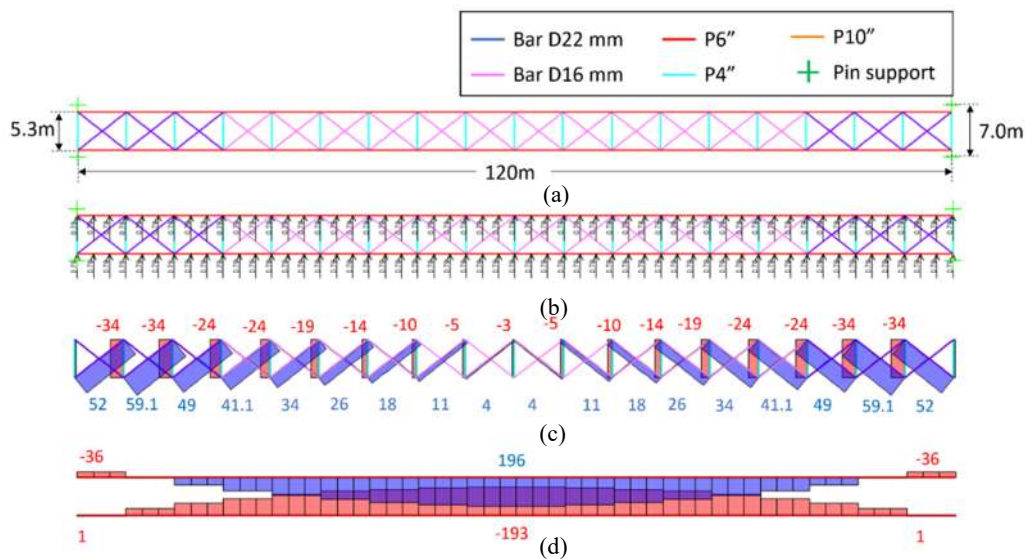


Figure 8. The conservative method of the lateral load resisting system control: (a) simplify structural geometry, (b) lateral load input (kN), (c) NFD wind bracing and longitudinal stiffener, and d) NFD of the one side P6'' member in the main arch system (kN).

Table 11. The wind bracing structural members safety control (force in kN)

Parameters	Wind bracing member section type	
	Bar D16 mm	Bar D22 mm
$T_u$	41.1	59.2
$\phi T_n$	72.4	136.9
$T_u/\phi T_n$	0.57	0.43

### Structural Lateral Resisting System Control

In the design phase, the conservative method was implemented to control the lateral load resisting system under stability issues, especially in the longitudinal direction of the coal shed structure. As explained in the introduction session, the lateral resisting system of the steel roof structure is configured with wind bracing and longitudinal stiffener as a struth and tie structural system. The resisting force contribution wind bracing member should be controlled appropriately. Because of the extremely slenderness of wind bracing, it is designed to resist tension forces only. Then, the longitudinal stiffener member is expected to resist the compression forces. The lateral resisting system was modeled with simplifying pinned-support plain truss system with 120 m of span, as illustrated in Figure 8 (a). There are two section types of wind bracing in the numerical model i.e., the bars with 16 mm (D16 mm) and 22 mm (D22 mm) of diameter. The frame element was assigned to all members with a release moment and tension only for the wind bracing. In the lateral loading input, we assumed that half of 10% of the dead load (D) is subjected to each structural joint. We assumed that the effective force of seismic load is 10% of the dead load, then the arch space-truss structural system will resist half of it. Furthermore, the other half of the effective force of seismic load is supported by this struth and tie structural system. The lateral loading input is depicted in Figure 8 (b). To consider tension only members, the numerical modeling should be conducted with non-linear analysis.

As the analysis result, the tension force occurrence of the wind bracing and the compression force of the longitudinal stiffener could be monitored, as depicted in Figure 8 (c). The struth and tie system in resisting the lateral load in a longitudinal direction could be formed as the expectation. Then, the edge member of the main arch space-truss (P6'') resists both the tension and compression forces following the axial stress distribution in the simple beam concept, as shown in Figure 8 (d). Finally, the most critical wind bracing members could comply with the safety criteria in resisting tension force, as shown in Table 11.

## 6. CONCLUSIONS

The design phase of the long-span coal shed structure has been conducted with implementing the structural safety criteria in the term serviceability and the ultimate state. The appropriate structural design concept, structural idealization, structural loading, structural analysis method, the interpretation of output, and structural member design

have been conducted with a thorough process. Then, considering non-linear geometry is also an important point in the design phase of the long-span coal shed structure related to the compatibility with the real structural displacement.

According to the structural analysis, the maximum displacement of the structural system under gravity and the lateral load of the wind and earthquake load are remaining below the standard limit. The largest displacement occurred in the case of wind load in the longitudinal direction. Based on the structural design with the LRFD method, the element members of the steel roof structure are fulfilled the safety criteria under the designed load. The most critical members occurred on P6" located at the middle span and P10" at the butt span under wind load and earthquake load, respectively. Furthermore, the analysis in the simplified model shows that the tension resistance of wind bracing bars are firm to resist transversal load in the longitudinal direction.

## REFERENCES

### Book

- AISC (2020) *Specifications for Structural Steel Buildings*, American Institute of Steel Construction. Edited by AISC. Chicago: AISC. DOI: 10.1061/taceat.0001170.
- ASCE (2017) *Minimum Design Loads and Associated Criteria for Buildings and Other Structures*. 7th–16th eds. Edited by S. E. Institute. Virginia: American Society of Civil Engineers.
- BSN (2006) *Standar Pembebanan untuk Jembatan*. Edited by Badan Standardisasi Nasional. Jakarta: Badan Standardisasi Nasional.
- BSN (2019) *Tata Cara Perencanaan Ketahanan Gempa Untuk Struktur Bangunan Gedung dan Non Gedung, Tata Cara Perencanaan Ketahanan Gempa Untuk Struktur Bangunan Gedung dan Non Gedung*.
- BSN (2020a) *Beban desain minimum dan kriteria terkait untuk bangunan gedung dan struktur lain*. Jakarta: Badan Standardisasi Nasional.
- BSN (2020c) *Spesifikasi untuk bangunan gedung baja struktural*. 1st edn. Jakarta: Nasional, Badan Standardisasi.
- Departemen Pekerjaan Umum (1987) *Pedoman Perencanaan Pembebanan Untuk Rumah dan Gedung 1987*. Jakarta: Yayasan Badan Penerbit PU.
- E. Bowles, J. (1997) *Foundation Analysis and Design Fifth Edition*. Fifth. The McGraw-Hill Companies, Inc. doi: 10.1007/978-1-349-13729-9\_26.
- FEMA (2020) 'NEHRP Recommended seismic provisions for new buildings and other structures', *Building Seismic Safety Council*, II(September), p. 388.
- Halmes, J. and Weller, R. (2002) 'HB 212 2002'.
- ICC (2017) *International Building Council 2018*. First Edi. Edited by I. C. Council. Illinois: International Code Council.
- IEA (2012) *Technology Roadmap High-Efficiency, Low-Emissions Coal-Fired Power Generation*. 9 PARIS CEDEX.
- IEA (2014) *Emissions Reduction through Upgrade of Coal-Fired Power Plants*. 9 PARIS CEDEX.
- Pustlitbang PUPR (2017) *Buku Peta Gempa 2017*. Cetakan Pe. Edited by Pusat Studi Gempa Nasional. Puslitbang PUPR.

### Journal

- Bhatt, M. S., and Labs, N. E. (2016) 'Effect of moisture in coal on station heat rate and fuel cost for Indian thermal power plants', *The Journal of CPRI*, 11(December), pp. 773–786.
- Hladik, P. and Lewis, C. J. (2010) 'Singapore National Stadium Roof Singapore National Stadium Roof', *International Journal of Architectural Computing*, 08(03), pp. 257–278.
- Yang, B. Y., and Asce, F. (1986) 'Stiffness matrix for geometric nonlinear analysis', *Journal of Structural Engineering*, 112(4), pp. 853–877. DOI: 10.1061/(ASCE)0733-9445(1986)112:4(853).

### Proceeding

- Du, W. *et al.* (2017) 'Design and optimization of the large span dry-coal-shed latticed shell in Liyuan of Henan province', in *Conferences, M. W. of (ed.) MATEC Web of Conferences*. MATEC Web of Conferences, pp. 1–7. DOI: 10.1051/mateconf/201710003024.